

Reconfigurable Liquid Crystal Reflectarray with Extended Tunable Phase Range

Saygin Bildik¹, Sabine Dieter², Carsten Fritzsche¹, Michael Frei²,
Christoph Fischer², Wolfgang Menzel², Rolf Jakoby¹

¹*Institute of Microwave Engineering and Photonics, Technische Universitaet Darmstadt,
Merckstr. 25, 64283 Darmstadt, Germany
bildik@imp.tu-darmstadt.de*

²*Institute of Microwave Techniques, University of Ulm, Albert-Einstein-Allee 41, 89081 Ulm, Germany*

Abstract—A coupled microstrip structure is investigated consisting of three fingerlike patches which are designed for liquid crystal technology. A unit cell based on the coupled structure is realized and characterized with a waveguide simulator. The proposed structure has a measured tunable phase range of 582°. It is used as an antenna element to design a reconfigurable reflectarray. The realized antenna is composed of 16x16 elements, and a slotted substrate integrated waveguide is used to illuminate it. Antenna patterns for desired main beam directions are synthesized at W-band with a developed Particle Swarm Optimization algorithm. Beam steering capability of the reflectarray is presented by steering the main beam to various angles applying the bias voltages obtained from the optimization algorithm.

I. INTRODUCTION

Microstrip reflectarray antennas stand out due to their planarity, low mass, low manufacturing cost and ease of fabrication compared to parabolic reflectors. Electronic reconfigurability adds another advantage to microstrip reflectarray antennas, since parabolic reflectors require mechanical scanning systems to change their main beam directions. Many methods based on varactor diodes [1], MEMS devices [2] and liquid crystals (LCs) [3], [4] have been experimentally demonstrated, in order to realize electronically reconfigurable reflectarrays. LCs are well-known as optical components of LCD monitors in which the optical anisotropy of LCs is used. On the other hand, anisotropy of LCs can be used to realize reconfigurable reflectarrays for at least up to 110 GHz with continuous tuning ability of array elements [5].

The inverted microstrip line topology is used to build a tunable antenna element. As depicted in Fig. 1a, the patches are printed on the upper substrate that is used as a superstrate, and another substrate whose upper part is completely metalized is used as ground plane. Between these two substrates a liquid crystal (LC) cavity is formed with the aid of spacers. The ground plane and one side of the superstrate where the patches are printed are coated by a mechanically rubbed thin polyimide film. This thin layer leads to a pre-alignment of the LC molecules parallel to the substrate surface and perpendicular to the RF field (see Fig. 1a). In this case, the relative permittivity of LCs is denoted as $\epsilon_{r,\perp}$. By applying a DC voltage between the patches and the ground plane (see Fig. 1b), the orientation of the molecules is changed leading to variations of the permittivity of the LC material.

The molecules will start to turn and, at the saturation point, are oriented almost parallel to the RF field. Thus, the parallel permittivity $\epsilon_{r,\parallel}$ becomes effective. This electronically controllable permittivity change is used to obtain different reflection phase values to design reconfigurable reflectarrays. In other words, different path lengths from the feed to an antenna element can be compensated, and the main beam can be steered to a desired direction by applying DC voltages to each element. DC voltages are applied with simple and thin bias lines which are in contact with patches. Compared to MEMS and varactor diodes, this biasing simplicity comes up with an advantage for the LC topology.

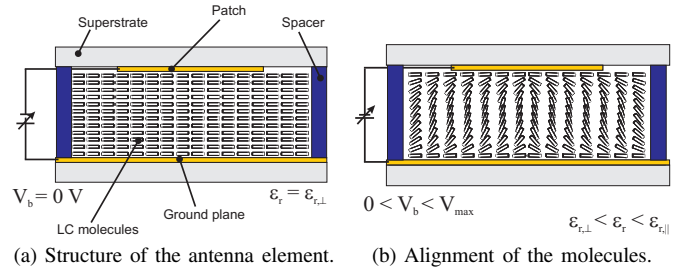


Fig. 1: Cross-section of the LC filled antenna element.

TABLE I: Specifications of the LC mixture at 30 GHz.

Mixture	$\epsilon_{r,\perp}$	$\epsilon_{r,\parallel}$	$\tan \delta_{\perp}$	$\tan \delta_{\parallel}$	Temperature
LC-C1	2.46	3.2	0.0131	0.0033	23 °C

II. UNIT CELL INVESTIGATIONS

Various shapes of microstrip patch elements have been examined in [6] by using a lumped-element model for the antenna elements. Furthermore, to extend the phase angle range of the antenna elements and to reduce the slope of the phase angles, coupled structures consisting of patches printed on a non-tunable substrate are presented in [7]. Within the aforementioned coupled structures, a 3-finger patch design (see Fig. 2b) is the most proper one for the LC technology in terms of biasing. The thin line connecting three patches to each other can be used as a part of a bias line.

In order to test the 3-finger patch topology for the LC technology, first of all antenna elements (unit cells) composed

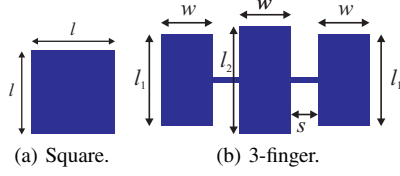


Fig. 2: Layouts of the investigated patches.

TABLE II: Dimensions of the designed patches.

l [mm]	l_1 [mm]	l_2 [mm]	w [mm]	s [mm]
1.01	0.975	1.025	0.5	0.2

of square and 3-finger patches have been designed for the LC mixture LC-C1 (see Table I). The square patch design is used as a reference structure for comparison, and dimensions of the designed patches are given in Table II. Additionally, a unit cell length of 2.14 mm ($0.55\lambda_0$ at 77 GHz) and a LC cavity thickness of $50 \mu\text{m}$ are set for the unit cells. As illustrated in Fig. 3, the 3-finger patch element has a 563° tunable phase range ($\Delta\varphi$) while the square patch element has 277° only at 77 GHz . A comparison can also be done in terms of another quantity named figure of merit (FoM) that is defined as $\frac{\Delta\varphi}{Max.loss}$. Although the 3-finger patch cell has higher losses, it has an FoM of $36.4^\circ/\text{dB}$ which is more than that of the square one ($33.8^\circ/\text{dB}$) due to the wider phase range.

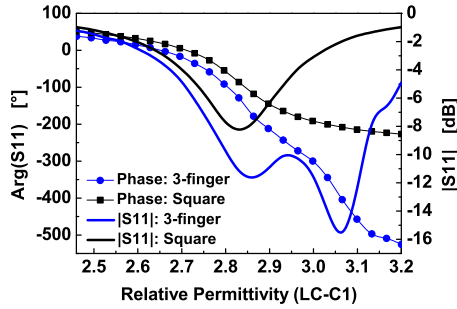


Fig. 3: Simulation results of the 3-finger and square patch elements.

As a second step to test the coupled structure, a unit cell based on the 3-finger patch is realized (see Fig. 4a) and characterized at W-band by using a waveguide simulator [8]. For biasing, a DC voltage from 0 V to 20 V is applied to the cell to obtain the phase shift. In accordance with the simulations, the manufactured unit cell has a $\Delta\varphi$ of 582° (see Fig. 4b). In comparison to the square patches, thus gaps in the phase adjustment can be avoided. Furthermore, since the coupled structure produces more than 360° of phase shift with the voltage range of 0 V to 20 V , not only the phases but also the amplitude variations of the elements can be taken into account within pattern synthesis. This can be performed by selecting necessary phase values with lower losses.

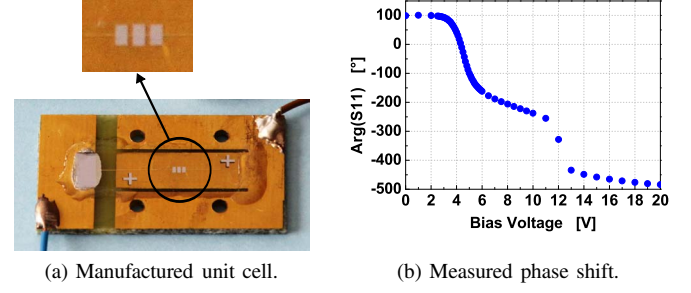


Fig. 4: Photograph and reflection phase of the realized unit cell.

III. ANTENNA DESIGN AND MANUFACTURING

A. Realization

After determining the 3-finger patch topology as antenna elements, a reconfigurable reflectarray based on LC technology is designed and realized. The fabricated antenna array consists of 16×16 patch elements with an element spacing of $0.55\lambda_0$. In order to tune the LC molecules, each 16 patches (on the same line) are connected by the same DC-bias lines. Therefore, the elements which belong to the same row yield the same phase, and hence the main beam of the reflectarray can be steered in one plane. For that reason, a feed with a line source characteristics is required to illuminate the antenna. As mentioned in section II, the bias lines are placed perpendicular to the resonant lengths l_1 and l_2 of the patch elements (see Fig. 5), and the width of the lines is set to $50 \mu\text{m}$ for the proposed topology to prevent interference with the RF field.



Fig. 5: Single row example of the reflectarray.

$300 \mu\text{m}$ -thick fused silica glass plates are used as substrates to carry the patch and ground plane electrodes (see Fig. 1a). In order to form the LC cavity, commercially available micro pearls with a diameter of $50 \mu\text{m}$ are used as cavity spacers. Micro pearls are mixed with glue and inserted between the two glass plates at the plate edges (outsides of the active region of the array) to form a $50 \mu\text{m}$ -thick cavity. However, a few small dots are also placed around the center of the array to obtain a uniform cavity height.

B. Characterization

After filling the reflectarray with the LC liquid (LC-C1), the antenna as shown in Fig. 6a (reflector part) is characterized by a quasi-optical lens setup [9]. Measurements are carried out by applying the same bias voltages (0 V to 20 V) to each antenna element row. Fig. 6b depicts the tuning capability of the realized antenna in terms of $\Delta\varphi$ measured as 546° at 77 GHz .

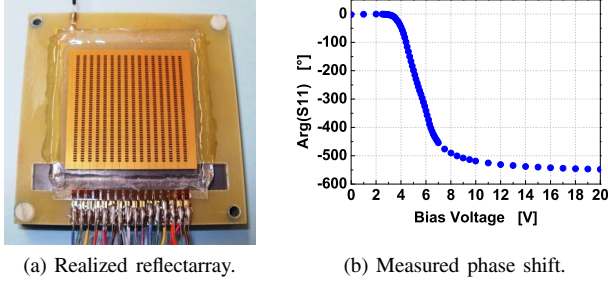


Fig. 6: Photograph and phase behavior of the realized antenna.

C. Antenna Feed

A feed based on a slotted substrate integrated waveguide (SIW, [10]) technology is used to illuminate the reflectarray. The simulation model and a picture of the feed are shown in Fig. 7. The SIW consists of a dielectric material with metallization on top and bottom. Its sidewalls are realized by rows of vias. In order to improve the sidelobe level, amplitude tapering is implemented by optimizing the slot widths and positions in the lateral direction. For the WR12-interface of the feed, a stepped transition from SIW to WR12 waveguide [11] with a matched 90° corner is used (see Fig. 7), optimized for frequencies around 77 GHz.

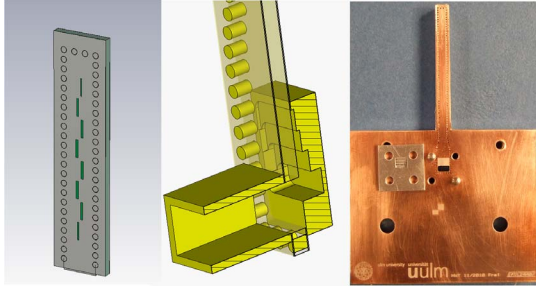


Fig. 7: Simulation model of the feed, cross section of the waveguide transition and photograph of the feed.

The measured far-field diagram of the slotted waveguide feed and the reflectarray antenna setup are illustrated in Fig. 8. Due to the one-dimensional reconfigurability in the E-plane, beam-forming is performed by the reflectarray. In the H-plane, the beam characteristic is obtained by the feed.

IV. ANTENNA PATTERN SYNTHESIS AND FAR-FIELD MEASUREMENTS

A synthesis method for folded reflectarray antennas using Particle Swarm Optimization (PSO) [12] was introduced in [13]. It is a combination of a powerful optimization algorithm with a method to decrease the amount of optimization parameters. A requirement for the procedure is an accurate extraction of the far-field diagram dependent on a certain reflector configuration whose pattern is evaluated and optimized.

The developed algorithm from [13] has been adapted within this work to optimize the reconfigurable patterns of

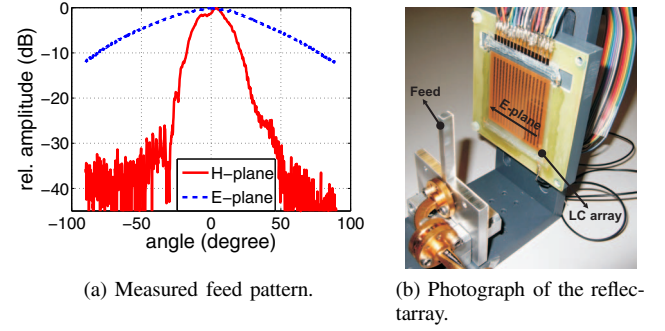


Fig. 8: Measured feed pattern and the reflectarray setup.

the fabricated reflectarray. The dependency of the elements' reflection behavior related to bias voltages is included into the calculations of the far-field diagrams. An array with 16×16 reflection elements is set up within the simulation, including the patch characteristics from the quasi-optical measurement results presented in section III. The phase distribution incident on the reflector and the illumination amplitude are included into the model by the measured feed pattern. Additionally, the line-wise adjustment of the array elements is considered.

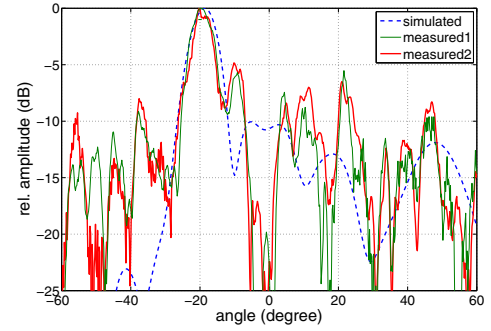


Fig. 9: Results of pattern synthesis and measurements at 77 GHz.

The pattern optimizations in this work are executed for a feed distance of 34 mm. Far-field measurements are accomplished in the anechoic chamber at 77 GHz by applying bias voltage combinations derived from the optimization algorithm explained above. A comparison between the synthesized reflectarray pattern and the far-field measurements for an offset beam angle at -20° is shown in Fig. 9. Additionally, Fig. 10 depicts the measurements of the realized array for three different main beam directions, 0° , -10° and -20° respectively. For the -20° beam, a second measurement has been carried out by flipping the voltage order calculated for the main beam at 20° as well as the diagram (see Fig. 9). The minor differences of these two measured curves show that the overall array seems to be quite homogeneous, although there are still overall phase and amplitude errors leading to deviations from the simulated diagram. These errors may result from more systematic fabrication tolerances (e.g. thickness

variations of the LC cavity of the array) and edge effects due to illumination of the array's edges.

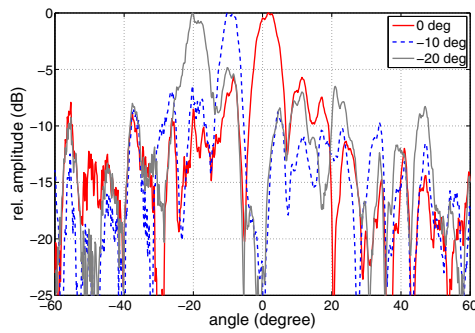


Fig. 10: Measured far-field patterns at 77 GHz.

In order to improve the measured patterns, phase errors caused by the fabrication tolerances can be reduced by using advanced technology processes. Thus, thickness variations of the LC cavity can be minimized. Furthermore, near-field measurements [14] will be performed; these data allow to characterize elements individually instead of the overall array characterization performed with the quasi-optical measurements. Thus, the characteristics of each antenna element can be used in the optimization routine.

In summary, however, the main lobe is successfully steered to desired angles as calculated by the optimization routine. Sidelobe levels of -5 dB for an offset beam angle of -20° and -7 dB for the angle of -10° are obtained. The steering ability of the antenna is not only limited to the above mentioned angles. The main beam can be also steered to wide angles continuously due to capabilities of the LC technology.

V. CONCLUSION

In this paper, a coupled microstrip structure is investigated based on three fingerlike patches for LC technology. A unit cell consisting of a 3-finger patch is realized and characterized with a waveguide simulator. Since the unit cell produces more than $360^\circ \Delta\varphi$ with a tuning voltage range of 0 V to 20 V, the proposed patch design is used as an antenna element to build a reconfigurable reflectarray. The realized reflectarray is composed of 16×16 elements, and a slotted waveguide feed based on SIW is used to illuminate the array. Antenna patterns for desired main beam directions are synthesized at 77 GHz based on a developed PSO algorithm. A quasi-optical measurement of the array has been performed to determine the necessary bias voltages. The one-dimensional beam steering capability of the reflectarray is demonstrated by successfully steering the main beam to 0° , -10° and -20° as calculated by the optimization algorithm. Phase errors caused by fabrication tolerances can be reduced by using advanced technology processes. Additionally, since near-field data can provide the opportunity of characterizing elements individually, possible errors in pattern synthesis may be reduced. Thus, the pattern of the realized antenna may be improved.

ACKNOWLEDGMENTS

Thanks are due to CST GmbH for providing CST Microwave Studio and Merck KGaA for providing the employed LCs. This work has been supported by the DFG-Project "Rekonfigurierbare Millimeterwellen-Antennen mit steuerbaren hoch-anisotropen Flüssigkristallen".

REFERENCES

- [1] S. V. Hum, M. Okoniewski, and R. J. Davies, "Modeling and Design of Electronically Tunable Reflectarrays," *IEEE Trans. Antennas Propag.*, vol. 55, no. 8, pp. 2200–2210, Aug. 2007.
- [2] H. Rajagopalan, Y. Rahmat-Samii, and W. A. Imbriale, "RF MEMS Actuated Reconfigurable Reflectarray Patch-Slot Element," *IEEE Trans. Antennas Propag.*, vol. 56, no. 12, pp. 3689–3699, Dec. 2008.
- [3] A. Moessinger, R. Marin, S. Mueller, J. Freese, and R. Jakoby, "Electronically reconfigurable reflectarrays with nematic liquid crystals," *Electronics Letters*, vol. 42, no. 16, pp. 899–900, Aug. 2006.
- [4] W. Hu, M. Y. Ismail, R. Cahill, J. A. Encinar, V. F. Fusco, H. S. Gamble, R. Dickie, D. Linton, N. Grant, and S. P. Rea, "Electronically Reconfigurable Monopulse Reflectarray Antenna with Liquid Crystal Substrate," in *Proc. Second European Conference on Antennas and Propagation EuCAP 2007*, Nov. 11–16, 2007, pp. 1–6.
- [5] S. Mueller, F. Goelden, P. Scheele, M. Witte, C. Hock, and R. Jakoby, "Passive Phase Shifter for W-Band Applications using Liquid Crystals," in *Proc. 36th European Microwave Conference*, Sep. 10–15, 2006, pp. 306–309.
- [6] M. Bozzi, S. Germani, and L. Perregrini, "A figure of merit for losses in printed reflectarray elements," *IEEE Antennas Wireless Propag. Lett.*, vol. 3, no. 1, pp. 257–260, 2004.
- [7] S. Dieter, C. Fischer, and W. Menzel, "Single-layer unit cells with optimized phase angle behavior," in *Antennas and Propagation, 2009. EuCAP 2009. 3rd European Conference on*, Mar. 23–27 2009, pp. 1149–1153.
- [8] A. Moessinger, R. Marin, J. Freese, S. Mueller, A. Manabe, and R. Jakoby, "Investigations on 77 GHz tunable reflectarray unit cells with liquid crystal," in *Antennas and Propagation, 2006. EuCAP 2006. First European Conference on*, Nov. 6–10 2006, pp. 1–4.
- [9] A. Moessinger, S. Dieter, W. Menzel, S. Mueller, and R. Jakoby, "Realization and characterization of a 77 GHz reconfigurable liquid crystal reflectarray," in *Antenna Technology and Applied Electromagnetics and the Canadian Radio Science Meeting, 2009. ANTEM/URSI 2009. 13th International Symposium on*, Feb. 15–18 2009, pp. 1–4.
- [10] L. Yan, W. Hong, G. Hua, J. Chen, K. Wu, and T. J. Cui, "Simulation and experiment on SIW slot array antennas," *Microwave and Wireless Components Letters, IEEE*, vol. 14, no. 9, pp. 446–448, Sep. 2004.
- [11] P. Feil and F. Bauer, "Two right-angle microstrip to waveguide transitions suitable for metal backed substrates," in *Electromagnetics in Advanced Applications (ICEAA), 2010 International Conference on*, Sep. 20–24 2010, pp. 450–453.
- [12] J. Kennedy and R. Eberhart, "Particle swarm optimization," in *Neural Networks, 1995. Proceedings., IEEE International Conference on*, vol. 4, 1995, pp. 1942–1948 vol.4.
- [13] S. Dieter, C. Fischer, and W. Menzel, "Design of a folded reflectarray antenna using Particle Swarm Optimization," in *Microwave Conference (EuMC), 2010 European*, Sep. 28–30 2010, pp. 731–734.
- [14] S. Dieter, A. Moessinger, S. Mueller, W. Menzel, and R. Jakoby, "Characterization of Reconfigurable LC-Reflectarrays Using Near-Field Measurements," in *German Microwave Conference, 2009*, Mar. 16–18 2009, pp. 1–4.